

UC San Diego

UC San Diego Previously Published Works

Title

Centrifuge Shake Table Tests on Rocking Footings on Sand

Permalink

<https://escholarship.org/uc/item/4g14w245>

Authors

Newgard, Jeffrey T

Hutchinson, Tara

McCartney, John S

Publication Date

2022-03-17

DOI

10.1061/9780784484043.061

Peer reviewed

Centrifuge Shake Table Tests on Rocking Footings on Sand

Jeffrey T. Newgard, P.E.¹, Tara Hutchinson, Ph.D., M.ASCE²,
John S. McCartney, Ph.D., P.E., F.ASCE²

¹ Department of Structural Engineering, University of California-San Diego, 9500 Gilman Drive, San Diego, CA 92093-0085; e-mail: jnewgard@eng.ucsd.edu, jthomasnewgard@gmail.com

² Department of Structural Engineering, University of California-San Diego, 9500 Gilman Drive, San Diego, CA 92093-0085; e-mail: tahutchinson@eng.ucsd.edu

³ Department of Structural Engineering, University of California-San Diego, 9500 Gilman Drive, San Diego, CA 92093-0085; e-mail: mccartney@ucsd.edu

ABSTRACT

This paper focuses on characterizing the cyclic behavior of a heavily loaded rocking footing supporting a bridge pier using centrifuge-model scale shake table tests. The intention of the test presented in this paper is to provide a baseline response for a footing that is expected to fail in the mode of rocking while supported on a uniform loose sand deposit. After presenting the details of the experimental setup and instrumentation plan, the results from a cyclic loading experiment are presented. Similar to the majority of tests in the FoRDy database, the footings investigated in this study were heavily loaded and experienced overturning failure.

INTRODUCTION

Shallow foundations provide the most cost-effective alternative to support bridge piers when structural loading conditions and scour potential allow. In addition to their low cost, shallow foundations may be designed such that they rock cyclically during an earthquake with the ground rather than the superstructure, developing a “plastic hinge”. It has long been understood that rocking footings dissipate energy once the underlying soil capacity is mobilized. This dissipated energy helps protect the integrity of the bridge superstructure, while also offering a natural tendency to re-center during an earthquake (Housner 1963). Recently, a body of experiments were dedicated within the databases, entitled Foundation Rocking in Cyclic (FoRCy) and Dynamic (FoRDy) Experiments to summarize measured test responses considering a variety of structure types, foundation sizes, and underlying soil conditions (Gavras et al. 2020).

There is a concern that these foundations will exhibit unacceptable movements during an earthquake, which has limited the adoption of rocking footing for bridge piers. Ground improvement has the potential to address this uncertainty by controlling the kinematics of the footing. A project underway at UC San Diego is focused on developing a database of centrifuge shake table tests on rocking footings resting on improved and unimproved sand layers which will

build upon the FoRCy and FoRDy experimental databases.

Ground improvement offers the means to not only control residual settlement and rotation after an earthquake event, but to strategically dissipate energy during one. The improvement techniques are aimed at controlling the kinematics with the intent of naturally recentering the footing and limiting the residual movement. Although the FoRCy and FoRDy experimental databases contains approximately 200 dynamic shaking tests, mostly performed in the centrifuge at model scale, only a few involved any form of ground improvement.

Although the overall study being performed at UC San Diego focuses on addressing the lack of tests on rocking footings on improved ground, this paper focuses on critical components of such a study including the development of the experimental setup, instrumentation plan, and procedures. This paper presents the results of a baseline test on unimproved sand that shows excessive deformations and ultimate failure to justify the need for using different ground improvement strategies. This paper also focuses on the rationale for selecting certain soil conditions, footing characteristics, and ground improvement strategy. The results from the baseline rocking footing focuses on the characteristic responses, including moment and settlement against structure rotation, for a simple single-degree-of-freedom type model footing and column assembly designed to scale in the centrifuge to a typical midsize highway prototype structure. A sequence of scenarios is performed to calibrate the loading protocol for the on-arm shaking table to reach the moment capacity of the footing.

TEST CONFIGURATION

Model Soil Conditions

Although ground improvement is commonly associated with liquefaction mitigation, for the present study it is instead aimed at controlling the kinematics of the rocking footing. For this reason, sand was pluviated into the laminar container in dry conditions as the focus of this study is on the response of the rocking foundation on weak soil but without the consideration of liquefaction.

In this study, Ottawa F-65 sand was chosen owing to its uniformity and thorough characterization in literature (e.g., Bastidas 2016; Zayed et al. 2017; Zayed et al. 2021). In developing the pluviation technique, passing the sand through a pair of sieves (No. 8 and No. 12) with the meshes oriented perpendicular to each other was found to disperse the sand uniformly. This method tended to produce deposits in the laminar container with relative density between 50% for a minimum drop height immediately above the deposit surface, to upwards of 85% for a maximum drop height of 0.6 m (about 24 in.) where the sand grains reached terminal velocity. Because a medium sand rather than a dense sand would be a more natural candidate for ground improvement in general, the sand was pluviated to a relative density of approximately 50%.

Footing Characteristics

Model footing characteristics were carefully selected considering 1) the wide body of literature available on dynamically loaded rocking footing tests (FoRDy), summarized in Gavras et al. (2020), and 2) typical prototype highway structures. A single-degree-of-freedom (SDOF) type model footing was chosen owing to its popularity in the database, as well as ease of assembly and reasonable approximation of a bridge's midspan footing-column subject to shaking in the transverse direction – that is, perpendicular to the long axis of the bridge deck. In this transverse direction, where the column is not restrained by the stiffer long axis of the bridge deck, both the SDOF model footing and full-scale column rock relatively freely. A schematic of the model footing and instrumentation is shown in Figure 1. Rationale for the test characteristics shown in this schematic is given below.

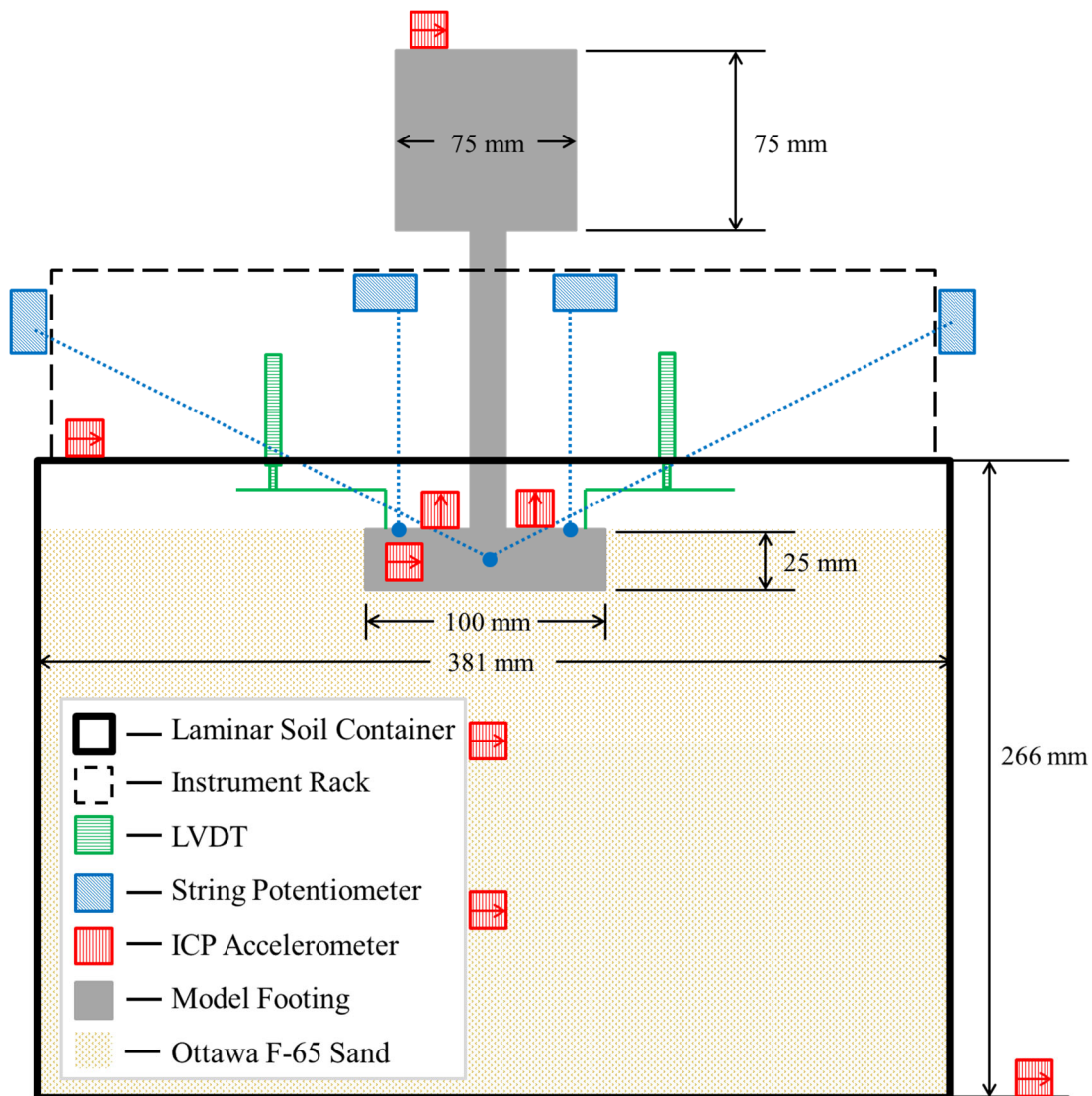


Figure 1. Schematic of model footing and instrumentation. All model scale units.

The three most important characteristics affecting the rocking behavior of a footing are 1) the magnitude of vertical load acting on the footing, especially relative to the footing's available bearing capacity as it rocks onto its side; 2) the height of the center of mass (H) of this vertical load above a footing with length (L); and 3) the aspect ratio of the footing. Each of these characteristics affecting the rocking behavior of a footing were considered in the design of the model rocking footing.

Regarding the first characteristic, special consideration must be given to the bearing capacity of a rocking footing because the contact area becomes smaller and therefore more intense as the footing rocks onto its side. The smallest contact area capable of supporting the vertical load – that is, when the vertical bearing capacity factor of safety (FS_v) is unity – is referred to as the critical area (A_c). Gajan and Kutter (2008) and Deng and Kutter (2012) provide a detailed description of the iterative calculation needed to determine A_c , which may be conveniently extended to the footing's moment capacity via the following relation:

$$M_{c,foot} = \frac{Q \times L_f}{2} \left[1 - \frac{A_c}{A} \right] \quad (1)$$

where $M_{c,foot}$ = moment capacity of the footing, Q = vertical load, L_f = footing length in the direction of rocking, A_c = critical area, and $A = L_f \times B_f$ = full area of the footing. A schematic depicting a rocking footing and these relevant terms is shown in Figure 2. Upon examination of a wide variety of tests in the FoRDy database, Sharma and Deng (2020) were able to group contours of cumulative footing rotation against settlement by the critical area. This finding makes perfect sense as a heavily loaded footing needing a larger critical area will have reduced moment capacity and therefore become susceptible to greater settlement at any given rotation magnitude during an earthquake event. A critical area ratio (A/A_c) of 5 has been chosen for the present study which is at the more heavily loaded side of all the tests in the FoRDy database, where A/A_c ranges between approximately 2 to 30.

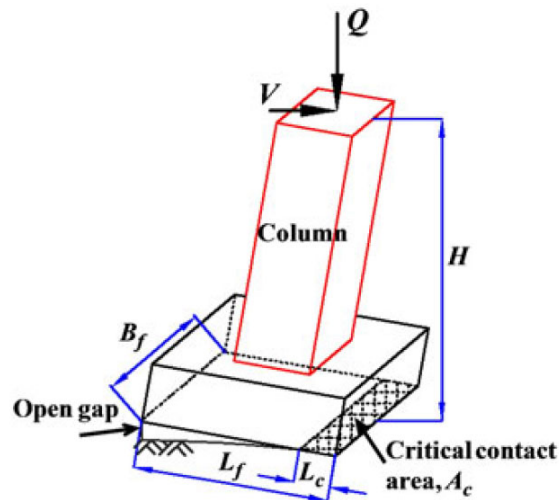


Figure 2. Schematic of rocking footing with relevant geometric variables (Deng et al. 2012).

Regarding the second characteristic, tests conducted by Deng et al. (2012) indicate that when H/L is at least 1 the footing will tend to rock. To ensure the onset of rocking, the center of mass representing the bridge deck for the SDOF model has been positioned at a height of 2L above the footing base for the present study.

Regarding the third characteristic, studies by Hakhamaneshi et al. (2013) determined that long, slender footings (along the rocking axis) tend to settle more than wide footings because the contact area of the slender footings mobilized a greater proportion of out-of-plane settlement during rocking. Naturally these long, slender footings would then be a stronger candidate for ground improvement to reduce settlements. For this reason, a model footing measuring 100 mm × 50 mm in plan area and 25 mm in depth, closer to a wall footing aspect but still representative of a typical highway bridge, was selected for testing. This model footing size allowed for approximately two times the footing length or width in distance, from footing edge to the laminar container walls, to reduce the chance of the container walls interfering with the bearing surface. A summary of test specifications is provided in Table 1, and a picture of the model footing and instrumentation assembled in the laminar soil container is shown in Figure 3. To balance the smaller size of the container and the need to minimize boundary effects, a centrifuge g-level of N = 25 was adopted in this study. The dynamic scaling relationships developed by Kutter (1992) were used in this study.

Table 1. Specifications for the centrifuge test performed at a scale factor of N = 50.

	Length of footing	Width of footing	Footing embedment	Height of bridge pier	Applied vertical load	Safety Factor for vertical loading	Critical area ratio	Bearing pressure	Moment / Vertical Load
	L_f (m)	B_f (m)	D_f (m)	H (m)	Q (N)	FS_v	A/A_c	q (kPa)	M/Q (m)
Model	0.1	0.05	0.025	0.2	27	7.0	5.0	5.5	1.2
Prototype	2.5	1.25	0.625	5.0	450e3	7.0	5.0	140	1.2

* Dimension and loading symbols listed are the same as those depicted in Figure 2.

Loading Equipment & Instrumentation

The model-scale rocking footing tests were conducted within a laminar container with externally supported laminates developed by Zayed et al. (2017), mounted on a servo-hydraulic ES-9 shake table on the 50 g-ton centrifuge at UCSD. The laminar container has 19 laminates which slide independently and provide a flexible boundary condition during shaking. The inside dimension of the laminates measures 381 mm × 241 mm in plan area and 266 mm in depth. Information regarding the initial configuration of the shake table and performance of the laminar container flexible boundary is available in Zayed et al. (2017).

Instrumentation includes sensors which track the footing's position and acceleration during shaking. Two linear variable displacement transducers (LVDTs) with DC output are oriented vertically and mounted on angle brackets connected to the footing. Because these sensors only have a 5 mm range, two string potentiometers are positioned similarly with mounts directly on the footing to check/backup the LVDT measurement should the footing settle beyond its stroke range. ICP-type accelerometers are mounted on the table, laminar container frame, footing, and within the sand to monitor dynamic forces imparted during shaking. These have sensitivities of either 1 V/g or 50 mV/g which can measure up to ± 5 g or ± 100 g, respectively.

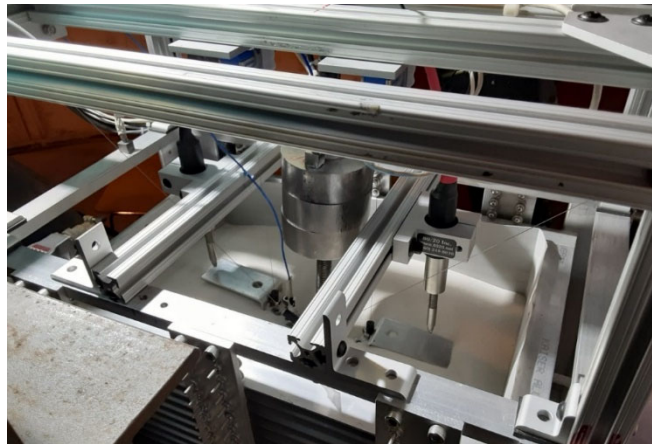


Figure 3. Model footing and instrumentation assembled in the laminar soil container.

PRELIMINARY RESULTS – ROCKING MODEL FOOTING ON UNIMPROVED SAND

The first step in the present study is to establish a dynamic loading protocol that will 1) cause the model footing to rock, and 2) exhibit excessive deformations requiring some type of ground improvement technique to better control the footing kinematics. Given the approximately 3 kg mass comprising the weight stack, elastic beam theory for a fixed base yields a natural frequency for the model footing of about 150 Hz. When considering soil-structure interaction effects via methods established in Veletsos and Meek (1974) the natural frequency is reduced to about 70 Hz. For the relatively tall, slender model footing under consideration, the rotational flexibility of the soil reduces the natural frequency more so than the translational flexibility. Given typical shear wave velocities (V_s) near 100 m/s, for recently placed Ottawa F-65 sand reported by Zayed et al. (2021), the natural frequency of the 250 mm high (H_{soil}) sand deposit in the laminar container would be approximately $4H_{soil} / V_s = 100$ Hz. Conveniently then, the sand deposit's natural frequency closely mirrors that of the model footing. However, the shake table experiences declining performance at frequencies above 70 Hz, so for the present study, shaking has been capped at this level. Nonetheless such a protocol balances the resonance desired between table, sand deposit, and footing, and table performance itself, and can reasonably be expected to induce sufficient rocking of the footing.

With the frequency characteristics sufficiently determined, the magnitude of shaking is all that is needed to load the footing to its moment capacity and induce yielding. According to Equation 1, the moment capacity of the prototype footing is approximately 400 kN-m. Dynamic moments are induced according to the product of the mass of any given component by its acceleration and mass centroid height above the footing base. The weight stack induces about 90% of the total dynamic moment compared to just 10% for the steel bar connecting it to the footing. The footing's settlement-rotation kinematic response, acceleration at the weight stack level, and induced moments relative to moment capacity of the footing are detailed in Figures 4 and 5. In Figure 4, the settlement (s) has been normalized by the footing width (B_f). The event depicted was one of a series of shakes and as such the settlement at the start of the event is nonzero.

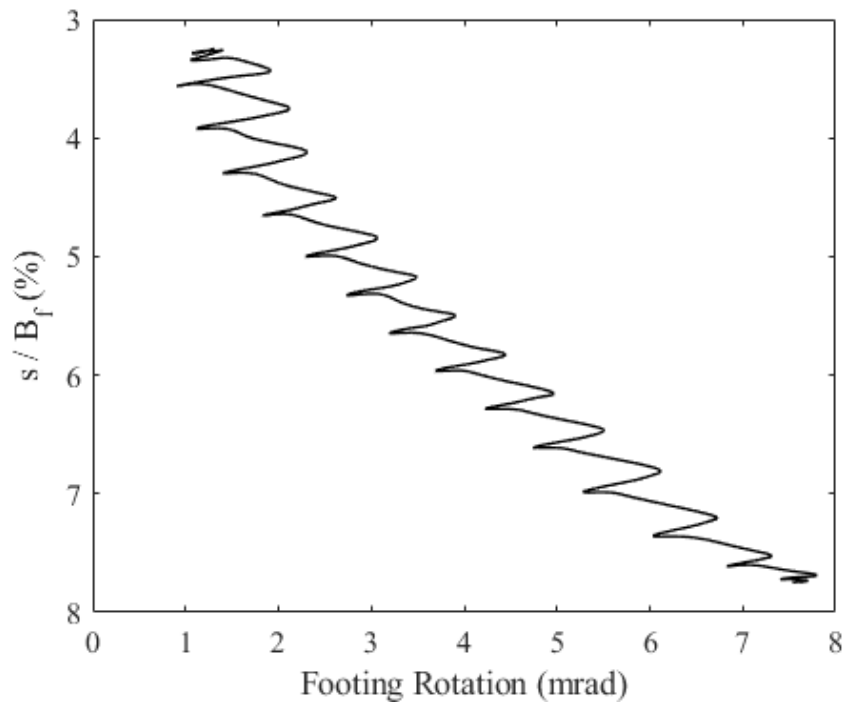


Figure 4. Footing kinematic response.

The footing settlement and rotation calculated by the two instrument types agrees well. The event depicted in these figures was the last of a series of 5 shakes at 50 Hz with duration of 0.5 s, with each shake gradually increasing in amplitude. This last event loaded the footing near its moment capacity, and indeed the footing yielded substantially during the event. Instead of recentering itself, the footing tipped further to one side as it settled. The result is consistent with the correlation made by Sharma and Deng (2020) illustrating a dramatic decrease in recentering ratio when A/A_c is at or below about 5. As such this baseline rocking footing configuration on unimproved sand is considered an appropriate starting point from which various ground improvement strategies will be applied to better control the footing kinematics.

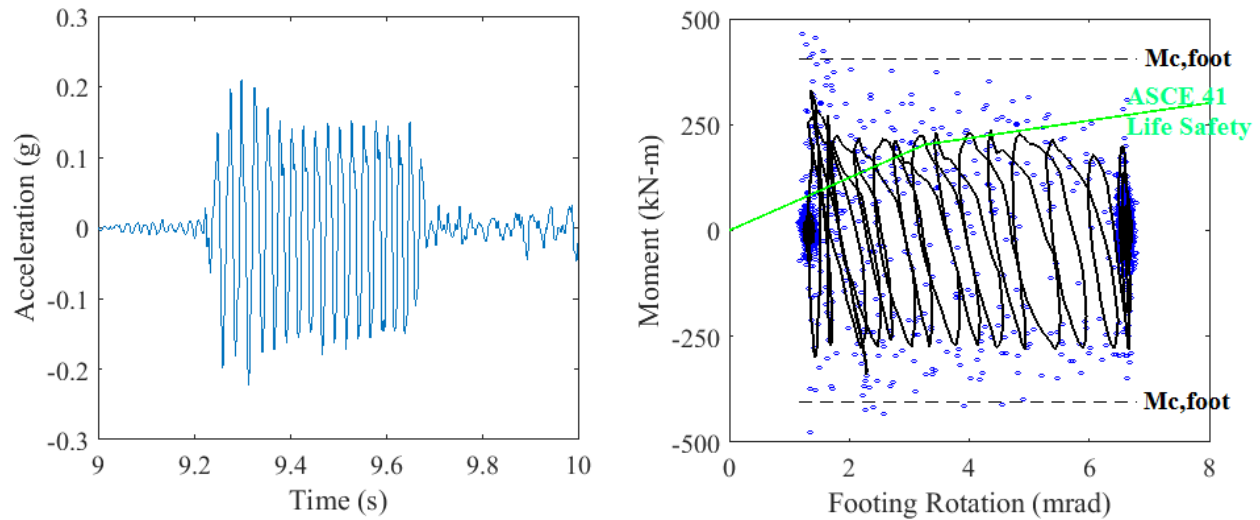


Figure 5. Dynamic moment induced during shaking and footing response.

TEST CONFIGURATION – GROUND IMPROVEMENT STRATEGY

A variety of studies are available cataloging the increase in bearing capacity obtained via ground improvement. Adams et al. (1997) placed geogrid and geocells in sand and found the bearing capacity to increase by about 2.5 times for the large-scale experiments studied. More specific to the application at hand, Anastasopoulos et al. (2012) suggested that only shallow soil improvement is needed because “rocking-induced soil yielding is only mobilized within a shallow layer underneath the footing”. Case histories like those in Arora et al. (2012) lend insight into typical California practices and the compression tests on field-mixed soil cement columns further guide construction techniques in the lab which mimic those in the field.

To match local practice, this study utilizes laboratory-mixed soil cement columns to control the kinematics of the rocking footing. Mix design for the columns was calibrated according to FHWA Publication No. HRT-13-046: Deep Mixing for Embankment and Foundation Support using the cement mass per total soil volume of 200 kg/m^3 reported by Arora et al. (2012). A water:binder (w:b) ratio of 3:1 was chosen to match typical lab-mixed specimens reported in the FHWA publication. Combined these parameters yield an as-mixed water content of 30% for the Ottawa sand. The mixture has been placed into molds measuring 25 mm in diameter and two columns will be placed along the lengthwise centerline on each side of the footing.

CONCLUSIONS

This study presented the details of a centrifuge modeling approach used to characterize the behavior of rocking footings, including the methodology to define the characteristics of the footing shape and static factor of safety to induce rocking during a given set of cyclic loading. As part of the development of this methodology, background on the advantages and large body of past work illustrating the reduction in structure damage via rocking footings has been presented. This body of work and the capabilities of the existing facilities at UCSD have been integrated to holistically determine appropriate loading protocols and model-prototype scaling for future rocking footing tests. The results for a baseline rocking footing on unimproved soil are presented in this paper, which will be compared in the future with the response of the same footing on sand layers with different ground improvement strategies. Future ground improvement strategies applied to the base case presented will aim to control the footing kinematics, limiting residual settlement and rotation, while still preserving an adequate degree of energy dissipation in accordance with the rocking footing design philosophy.

ACKNOWLEDGEMENTS

The present study is funded by the Pacific Earthquake Engineering Research (PEER) Center and their support is greatly appreciated. The views are those of the authors alone.

REFERENCES

- Adams, M.T. and Collin, J.G. (1997). "Large model spread footing load tests on geosynthetic reinforced soil foundations." *Journal of Geotechnical and Geoenvironmental Engineering*, 123(1), 66-72.
- Anastasopoulos, I., Kourkoulis, R., Gelagoti, F., and Papadopoulos, E. (2012). "Rocking response of SDOF systems on shallow improved sand: An experimental study." *Soil Dynamics and Earthquake Engineering*, 40, 15-33.
- Arora, S., Shao, L., and Schultz, J.M. (2012). "Wet Soil Mixing for Bearing Capacity, Liquefaction Mitigation, and Water Cutoff for Scour Protection for a New Bridge Abutment." *Grouting and Deep Mixing*, 575-584.
- Bastidas, A.M. (2016). *Ottawa F-65 Sand Characterization*. Ph.D. Thesis, University of California-Davis.
- Deng, L, Kutter, BL, and Kunnath, SK (2012). "Centrifuge modeling of bridge systems designed for rocking foundations." *Journal of Geotechnical and Geoenvironmental Engineering*, 138(3), 335–344.
- Deng, L. and Kutter, B.L. (2012). "Characterization of rocking shallow foundations using centrifuge model tests." *Earthquake Engineering and Structural Dynamics*, 41 (1), 1043-1060.

- Gajan, S. and Kutter, B.L. (2008). “Effect of critical contact area ratio on moment capacity of rocking shallow footings.” *Geotechnical Earthquake Engineering and Soil Dynamics IV*, Sacramento, California.
- Gajan, S. and Kutter, B.L. (2008). “Capacity, settlement, and energy dissipation of shallow footings subjected to rocking.” *Journal of Geotechnical and Geoenvironmental Engineering*, 134 (8), 1129–1141.
- Gavras, AG, Kutter, BL, Hakhamaneshi, M, Gajan, S, Tsatsis, A, Sharma, K, Kohno, T, Deng, L, Anastasopoulos, I, and Gazetas, G (2020). “Database of rocking shallow foundation performance: Dynamic shaking.” *Earthquake Spectra*, 36 (2), 960-982.
- Hakhamaneshi, M., Kutter, B.L., Tamura, S., Gavras, A.G., Liu, W. and Deng, L. (2013). “Rocking foundations with different shapes on different soils.” *10th CUEE*, Tokyo, Japan.
- Hakhamaneshi, M., Gavras, A.G., Wilson, D.W., Kutter, B.L., Liu, W., and Hutchinson, T.C. (2014). “Effect of footing shape on the settlement of rectangular and I-shaped rocking shallow foundations.” *ICPMG 2014*, Perth, Australia.
- Housner, G.W. (1963). “The behavior of inverted pendulum structures during earthquakes.” *Bulletin of the Seismological Society of America*, 53 (2), 403-417.
- Kutter, B.L. (1992). “Dynamic centrifuge modeling of geotechnical structures.” *Transportation Research Record*. 1336.
- Sharma, K and Deng, L. (2020). “Field testing of rocking foundations in cohesive soil: cyclic performance and footing mechanical response.” *Canadian Geotechnical Journal*, 57 (6), 828-839.
- Veletsos, A.S. and Meek, J.W. (1974). “Dynamic Behaviour of Building-Foundation Systems.” *Earthquake Engineering and Structural Dynamics*, 3, 121-138
- Zayed, M., Luo, L., Kim, K., McCartney, J.S. and Elgamal, A. (2017). “Development and performance of a laminar container for seismic centrifuge modeling.” *Performance Based Design in Earthquake Geotechnical Engineering, III*, Vancouver, British Columbia.
- Zayed, M., Ebeido, A., Prabhakaran, A., Kim, K., Qiu, Z. and Elgamal, A. (2021). “Shake Table Testing: A High-Resolution Vertical Accelerometer Array for Tracking Shear Wave Velocity.” *Geotechnical Testing Journal*, 44 (4), 1097-1118.